JOURNAL OF MATERIALS SCIENCE 4 (1969) 789–796

The Morphology and Growth of Creep Cavities in α-iron

A. L. WINGROVE
Defence Standards Laboratories, Alexandria, New South Wales, Australia

D. M. R. TAPLIN
Materials Science Laboratories, University of Waterloo, Ontario, Canada

Received 27 February 1969, and in revised form 23 June

Electron fractography has been used to study the intergranular cavities formed in alpha-iron during slow tensile deformation at high temperatures. A minimum in ductility is observed at about 700° C: this coincides with conditions where grain-boundary sliding makes a maximum contribution to the overall deformation and where the morphology of the cavities tends to be dendritic and finely terraced. This is explained in terms of the gradient of chemical potential for vacancies which may develop at the cavity periphery during grain-boundary sliding. Under other testing conditions, planar growth is observed and the cavity surface is often faceted.

1. Introduction

This paper is concerned with the growth of the intergranular cavities which are generated during slow tensile deformation at about half the melting temperature. Baluffi and Siegle [1] showed that vacancies will condense at cavities when the tensile stress acting across the boundary is sufficient to overcome the tendency of the cavity to shrink under the influence of surface tension. The model envisages atom transfer from the cavity to the boundary via grain-boundary diffusion, and several quantitative analyses have been carried out [2–4]. The main problem is in determining the gradient of chemical potential for vacancies at the periphery of the cavity. This may have been underestimated because the vacancy concentration in the boundary is likely to be enhanced if sliding is occurring. Specifically, the grain-boundary dislocations causing sliding will probably interact with one another, creating vacancies. Also, according to the model of Ishida and McLean [5], dislocations will move non-conservatively along the boundary, emitting vacancies. It follows that the rate of cavity growth will be enhanced. This approach is important, in so far as it relates grain-boundary sliding to cavity growth [6].

The vacancies arriving at the cavity will tend to be redistributed in order to reduce the total surface energy. The diffusion flux (J_S) for this process of redistribution depends upon the surface diffusion coefficient and the rate of change of the radius of curvature [7]. It is usually assumed that J_S is much greater than J_B, where J_B is the vacancy flux into the cavity, so that the cavities maintain an equiaxed shape during growth. It is then possible to calculate expressions for both time and elongation to fracture (e.g. [8]). When J_S is reduced by surface adsorption, and under conditions of high stress when J_B would be increased, it is possible for the cavities to grow laterally. This situation has been considered by Yamazaki [9]. Furthermore, when the cavity reaches a certain critical size it may propagate according to Griffith-Orowan conditions [10]. There are thus several reasons for thinking that existing expressions underestimate the cavitation rate.

Several other mechanisms have been suggested for growth. Cavities may increase their area as a shear crack, under the direct influence of grain-boundary sliding. This process would be most effective on grain-boundaries situated at an angle to the tension direction. There is also a mechanical process giving maximum growth on boundaries normal to the tension direction. The

tensile stress concentration at cavity apices may induce plastic flow or break bonds directly.

To distinguish which particular process is dominating, it can be helpful to study the angular distribution of cavities with respect to the tensile axis. Gittins and Williams [11] have done this for copper and concluded that at very slow deformation rates (10^{-5} h^{-1}) the Baluffi-Siegle model predominates, whilst with increasing deformation rate (10^{-1} h^{-1}) growth is controlled by grain-boundary shearing. Fig. 1 shows some similar results on alpha-brass where the variable of grain size is examined [12]. The inference here is that at fine grain sizes shearing plays an important rôle in cavity growth, whilst at coarse grain sizes, processes which involve a normal stress dominate. Metallography indicated that the cavities were in the form of sharp disc-shaped cracks so that the transition in growth mechanism here may have been between the two mechanical processes discussed above. This emphasises further the importance of detailed studies of cavity morphology.

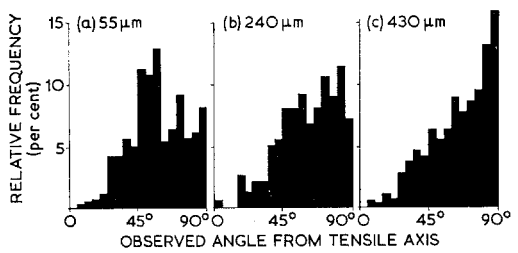

Figure 1 Relative frequency plots of the observed angular distribution with respect to the stress axis of cavities in alpha-brass of three average grain diameters (a) 55 μm, (b) 240 μm, (c) 430 μm, strained at 450° C and 10^{-2} h^{-1} in argon [12].

2. Experimental

Iron containing (wt %), 0.042 O, 0.05 N, 0.005 C, 0.002 Mn was used. Round (3.2 mm diameter) tensile specimens (gauge length 12.7 mm) were machined from swaged rod and annealed in vacuum to give a stabilised grain size of 95 μm average diameter. Tests were carried out in an argon atmosphere using modified Hounsfield Tensometers which extended specimens with a constant nominal strain-rate. Some dead-load creep tests were also done. Grain-boundary sliding measurements were made by measuring the mean height of surface steps perpendicular to the tensile axis; boundaries were sampled by working along longitudinal traverses. A focusing technique was used and it was possible to determine a step height to $\pm$ 0.5 μm. A measure of the contribution of grain-boundary deformation (ϵ_{gb}) to the total strain was obtained by taking the product of the mean step height ($\bar{v}$) and the number (n) of grain-boundaries per unit length (i.e. taking $k = 1$ in the formula, $\epsilon_{gb} = n\bar{v}k$). Density change was measured on the gauge length of specimens by a hydrostatic displacement method. For these experiments, longer specimens were used to improve accuracy; these had a gauge length of 38 mm with a cross-section of 4.5 mm diameter and a grain size of 180 μm.

The iron used fractures in a brittle intercrystalline manner at low temperatures. After testing, specimens were quickly cooled to room temperature, notched and fractured so that the cavities were dissected in the plane of the boundary. By platinum-carbon replication followed by electron microscopy, an accurate three-dimensional view, giving details of the cavity profile in the boundary plane and the shape of the cavity surfaces, was obtained [13]. By tilting the replica and taking photographs of stereo-pairs it was possible to analyse the cavity morphology in detail [14]. Observations were also made using optical metallography and a scanning electron microscope in which similar but less clear results were obtained.

3. Results

The relationships between total elongation at fracture and test temperature for tests at three strain-rates are recorded in fig. 2. In a separate series of tests, using longer specimens, the minimum in ductility and maximum cavitation,

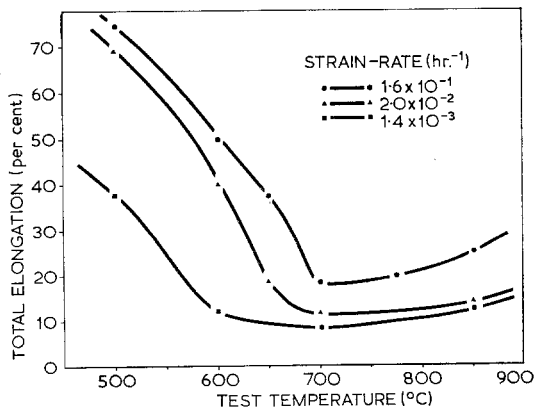

Figure 2 The relationship between test temperature and elongation at three strain-rates (gauge length 12.7 mm).

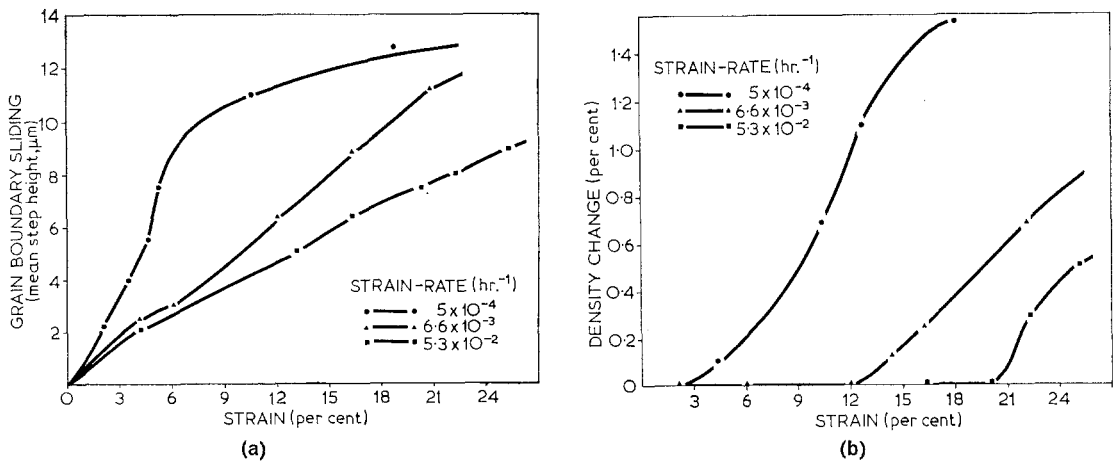

Figure 3 The relationship between (a) strain and grain-boundary sliding (mean surface step height), (b) strain and density change, tested at 700° C and three strain-rates (gauge length 38 mm).

was found to be associated with a maximum contribution of grain-boundary sliding (measured at the fracture strain) to the overall deformation (table I). Some grain growth occurred in tests at 850° C and the extent of necking increased, indicating that the final fracture stage was made more difficult.

TABLE I

Temperature ° C	Strain-rate h^{-1}	Grain-boundary sliding (% contribution at fracture ~ 20% strain)	Density decrease %
600	5.0×10^{-2}	8.5	0.40
	6.6×10^{-3}	18.5	0.44
700	5.0×10^{-2}	20	0.50
	6.6×10^{-3}	28	0.68
	5.3×10^{-4}	39.5	1.53
850	5.0×10^{-2}	17.5	0.53
	6.6×10^{-3}	21.5	0.63
	5.3×10^{-4}	23	1.05

Figs. 3a and b demonstrate that the onset of cavitation as shown by a change in density does not coincide with the onset of sliding (note that different gauge length specimens were used here so that the strain rates in fig. 3 do not correspond exactly with those in table I). It is clear from an examination of these results that a combination of sliding, time, stress and strain are involved in the cavitation process.

Electron photomicrographs of grain-boundary surfaces containing cavities are shown in figs. 4 to 11. The observations are confined to the

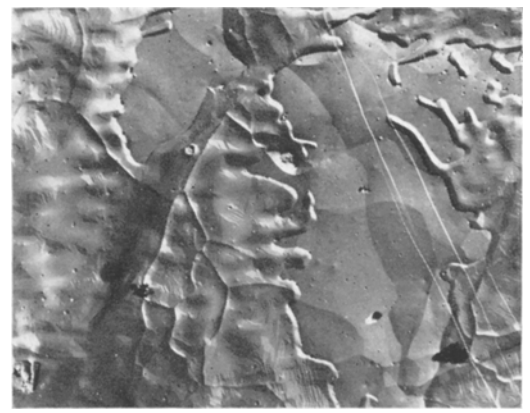

Figure 4 Large area of grain-boundary cavitation showing undulating cavity profile, terracing and marked grooving at intersections of sub- and grain-boundaries with the cavity surface. Strained at 700° C and 1.6×10^{-1} h^{-1} (× 1100).

morphology of growth rather than nucleation because no major difference in cavities nucleated at different sites was found. A wide range of shapes was observed. The cavity was either faceted (fig. 10) or curved (fig. 7). On a smaller scale the surface was often terraced (figs. 5 and 6). The profile of the cavities in the plane of the grain-boundary also varied. Sometimes a definite planar interface was obtained so that the profile of the cavities was either rounded or regularly crystallographic on a particular boundary plane (fig. 7). Under certain conditions undulations were observed at the interface between the cavity and the grain-boundary (fig. 4). Sometimes (figs.

Figure 5 Dendritic cavity profile with rounded surface and curved terraces. Strained at 850° C and 1.6×10^{-1} h^{-1} ($\times$ 4000).

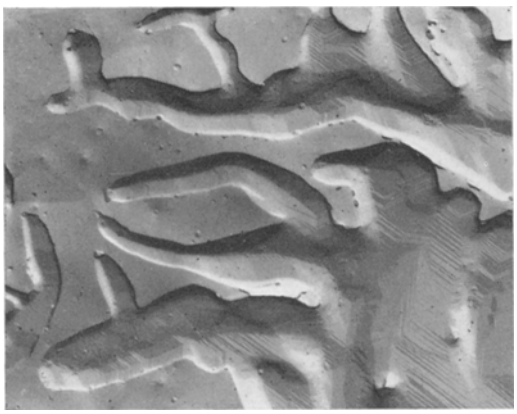

Figure 6 Marked dendritic growth in boundary plane with fine-scale terraces and some polyhedral facets. Strained at 700° C and 2×10^{-2} h^{-1} ($\times$ 5500).

5 and 6) this type of profile became markedly "dendritic".

Several other features were apparent. In fig. 4 it is possible to distinguish marked grooving

Figure 7 Planar cavity growth with smooth surface and some curved terraces showing three-fold symmetry of growth on boundary plane. Strained at 850° C at 2×10^{-2} h^{-1} ($\times$ 1030).

where sub-boundaries and grain-boundaries intersect the cavity surface. Fig. 9 shows parallel "gouge" markings on sections of the grain-boundary free of cavities, possibly due to sliding in this direction; the cavities themselves exhibit crystallographic symmetry.

A preliminary classification of these features with respect to test-temperature and strain-rate is possible. At 600° C the cavity surface was generally found to be markedly polyhedral with large facets. Terraces were observed in the form of relatively large well-shaped steps. At 700° C the cavity surface was finely terraced with some degree of faceting. At this temperature the cavity profile was often dendritic (fig. 6). At 850° C the surface of the cavity was rounded and the terraces were also curved. At this temperature dendritic growth was only observed at the fastest strain-rate (fig. 5); with decreasing strain-rate the interface was again planar, sometimes with a rounded and sometimes a regular crystallographic profile (fig. 7). A general classification over a typical range of conditions is given in table II.

Perhaps the dendritic mode of growth is the most striking feature of these observations. For particular conditions of testing the dendritic arms seem to have a characteristic spacing and minimum radius of curvature in the boundary plane. Interrupted tests suggested that the dendritic mode of growth only develops after the cavities have reached a certain size. This is reasonable if the arms have a minimum radius of curvature and therefore thickness; perhaps the cavity in fig. 8 has just reached this critical size. The dendritic morphology also seems to be

TABLE II

Strain rate	Temperature ° C		
	600	700	800
1.6×10^{-1}	large polyhedral facets with some terracing	some facets with fine-scale terraces and undulating cavity profile (fig. 4)	rounded surface with wavy fine-scale terraces, dendritic profile (fig. 5)
2×10^{-2}	polyhedral facets with terracing	polyhedral facets with fine-scale terraces, marked dendritic profile (fig. 6)	rounded surface with wavy terraces, planar interface, sometimes crystallographic profile (fig. 7)
1.4×10^{-3}	polyhedral facets with terracing	polyhedral facets with fine-scale terraces, dendritic profile (fig. 8)	rounded surface with planar growth and rounded profile

associated with the existence of fine-scale terracing.

Cavities were not often observed to be equiaxed in shape; this was only found for quite small cavities (e.g. less than 2 μm diameter). In general the cavities were shallow, i.e. their smallest dimension was that perpendicular to the boundary plane, especially under conditions of minimum ductility (figs. 6 to 8). This is consistent with the model of Yamazaki [9]. By use of stereometry [14] it was possible to analyse the crystallography of the facets on the cavity surfaces. One example with the faces indexed is shown in fig. 10. In general, four types of faces were observed: {100}, {110}, {102}, {112}, and in each case examples were obtained of large flat faces without terracing, so that the planes are probably true planes rather than combinations of planes. The relative areas of the planes of various indices suggest that the {100} planes have the lowest surface energy. This is the plane of cleavage for iron. The crystallography of the terraces could not be specifically determined

Figure 9 Cavity showing terracing and preferred growth direction with "gouge" markings on the uncavitated grain-boundary surface, strained to 6% extension at 700° C and 5% 10^{-4} h^{-1} (× 4400).

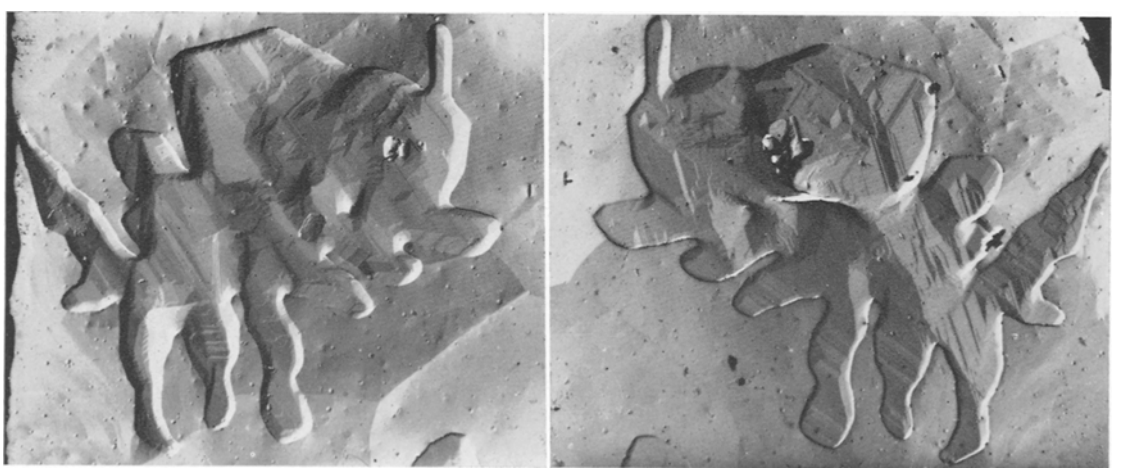

Figure 8 Matching halves of a cavity from both sides of the fracture; onset of dendritic growth with fine-scale terraces and faceted areas. Strained at 700° C at 1.4×10^{-3} h^{-1} (× 1900).

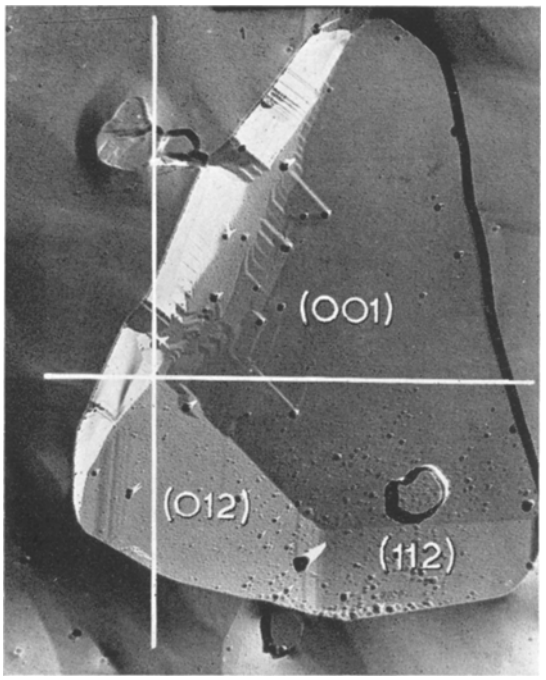

Figure 10 Cavity with planes of facets and depth determined by stereometry. Strained to 6% extension at 700° C and 5×10^{-4} h^{-1} ($\times$ 10000).

because the size of the steps was too small for the use of the stereo technique.

After testing, some specimens were annealed in vacuum. Table III records the change of density of specimens deformed 16% at 700° C and 6×10^{-3} h^{-1} with annealing.

TABLE III

Annealing time h	Density increase % 700° C	850° C
0	0.215	0.271
50	0.184	0.240
100	0.163	0.231
200	0.146	0.226
500	0.140	0.226

After 500 h at temperature, grain growth was considerable so that many of the cavities became isolated within the grains. This is probably the main factor limiting the complete sintering of the cavities. Fractographic examination of these specimens revealed that the cavities present had become somewhat more equiaxed but remnant dendritic features were still present. Cavities annealed at 700°C were generally polyhedral with faceted surfaces (fig. 11a) whilst cavities annealed at 850° C had curved surfaces (fig. 11b). This suggests that the observations with respect to cavity surface summarised in table II, represent conditions close to equilibrium.

Cavities produced by dead load creep under similar conditions of maximum stress and rate of deformation could generally be classified according to the observations summarised in table II. It was possible to rationalise the results obtained from both types of test according to a Zener-Holloman creep equation. The general trends of temperature and strain-rate upon ductility were similar for each type of test but the actual values

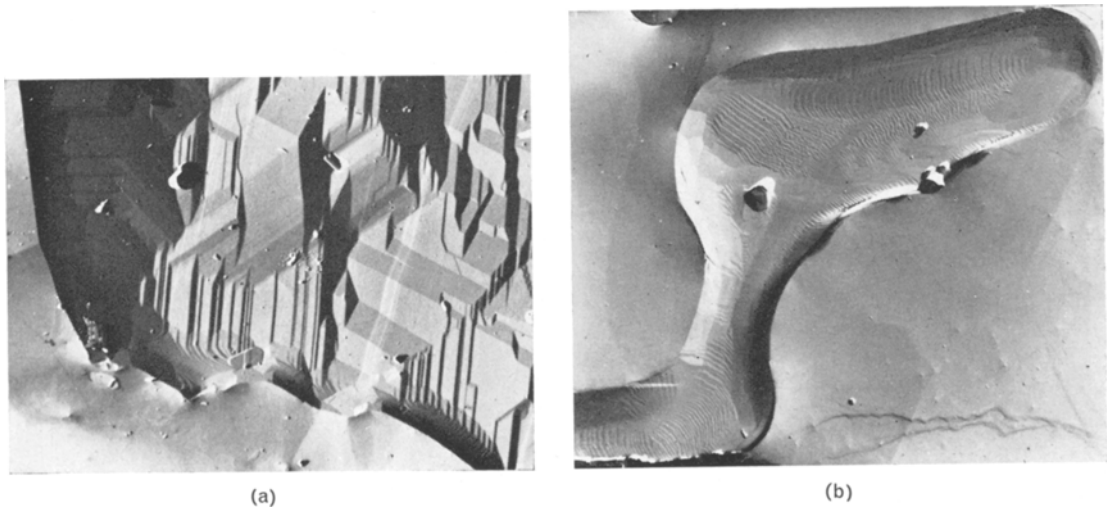

(a) (b)

Figure 11 Cavities from specimen strained at 700° C and 6×10^{-3} h^{-1} followed by annealing for 500 h at 700° C (a) ($\times$3200), and 850° C, (b) ($\times$ 2600).

of elongation to fracture for comparable test conditions varied considerably. For example, at 700° C and a stress of 1.7 kg/mm² the creep test gave an elongation of 32% with a secondary creep rate of 6×10^{-3} h^{-1}, whilst a constant strain-rate test at 1.4×10^{-3} h^{-1} gave an elongation of 9% with a maximum stress of 1.7 kg/mm².

4. Discussion

The cavities observed were generally of a form which is most readily explained in terms of mechanisms of growth involving the condensation of vacancies. However the theory of Baluffi and Siegle [1], as developed by Speight and Harris [4] and Yamazaki [9] remains inadequate to explain the observations.

The first theoretical assumptions to examine are those involved in the calculation of the gradient of chemical potential for vacancies. In the present work there is a close association of grain-boundary sliding with the maximum overall rate of cavitation (minimum ductility). This can be explained if the sliding generates a higher gradient of chemical potential by contributing to the vacancy concentration between the cavities, or by enhancing the coefficient for diffusion of vacancies along the boundary. In these circumstances, the gradient of chemical potential may be so large that the tendency for perturbations in the interface to continue growing preferentially into the region of increasing vacancy concentration, is greater than the restricting force of surface tension. This instability condition gives rise to a dendritic growth morphology as is observed during solidification and other transformations. The early stages of dendritic growth seem to involve the formation of sinusoidal shape perturbations as observed in solid state precipitation by Malcolm and Purdy [17]. Quantitative studies of these are envisaged following the analysis of Mullins and Sekerka [18].

A natural consequence of the dendritic growth is that the overall rate of transformation is expected to be much faster than during planar growth. In the present process, dendritic growth would be expected under conditions of high stress and high rate of grain-boundary sliding. At low temperatures and high strain-rates, where grain-boundary sliding does not contribute significantly to deformation, and at high temperatures and low strain-rates, where the vacancy concentration gradient would be reduced a planar mode of growth would be expected. This approach is in accord with the present observations.

The second assumption in the general theory to question is that the cavities maintain an approximately equiaxed shape. Quite apart from the dendritic effect, this is clearly not valid for the present conditions where the cavities are generally shallow. The surface diffusion current is apparently insufficient to spheroidise the cavities as they grow: Yamazaki [9] has now analysed this situation.

The next question to consider is the crystallographic features of the cavities. The most likely explanation of the terraces is that they are manifestations of a step-wise growth process. Mullins and Hirth [15] have developed the kinetic theory of step-motion in growth processes based on the original analysis by Frank. In principle this theory is directly applicable to the present situations and it would be expected, for example, that the rate of growth would depend on step-density and time-dependent impurity adsorption on to the steps [15]. This gives some understanding of why the most closely spaced and well-defined steps are associated with the dendritic growth and gives a pointer for future work. The terraces may later merge together to produce the large facets observed on the cavity surfaces (fig. 10). The facets also develop directly during growth under planar conditions. The rate of vacancy condensation under these slow growth conditions will be different for different crystal planes. The result will be polyhedral cavities of the same form as crystals growing in the vapour under minimum surface energy conditions. This situation has been analysed recently for cavities in a body-centred-cubic structure by Farrell, Loh and Stiegler [16] and the present results are in close agreement with this work. The annealing experiments suggest that the faceted surface represents the equilibrium conditions for growth at 700° C. At 850° C it seems that the equilibrium shape is not a polyhedral but a rounded cavity. The crystallographic symmetry of the cavities in fig. 8a are more difficult to explain since the symmetry is with respect to the grain-boundary itself. Similarly, there have been some indications that the preferred direction of growth of the dendritic arms is sometimes controlled by crystal symmetry. Both these effects probably occur at grain-boundaries with specific misorientations, which have certain crystal planes coincident.

Acknowledgement

The work has been supported by the Australian Atomic Energy Commission and the National Research Council of Canada. The material was supplied by the British Iron and Steel Research Association. Much of this work was carried out in the Department of Metallurgy, University of Melbourne and we are grateful to Dr R. C. Gifkins and Professor M. E. Hargreaves for encouragement.

References

1. A. W. BALUFFI and L. L. SIEGLE, *Acta Met.* **5** (1957) 449.
2. D. HULL, and D. E. RIMMER, *Phil. Mag.* **4** (1959) 673.
3. R. T. RATCLIFFE and G. W. GREENWOOD, *ibid* **12** (1965) 59.
4. M. V. SPEIGHT and J. E. HARRIS, *Met. Sci. J.* **1** (1967) 83.
5. Y. ISHIDA and D. MCLEAN, *ibid* 171.
6. D. MCLEAN, *Rep. Prog. Phys.* **29** (1966) 1.
7. C. J. HERRING, *J. Appl. Phys.* **21** (1950) 437.
8. R. P. SKELTON, *Phil. Mag.* **15** (1967) 405.
9. M. YAMAZAKI, National Research Institute for Metals, Tokyo, Japan (1968).
10. D. M. R. TAPLIN, *J. Aust. Inst. Met.* **10** (1965) 336.
11. A. GITTINS and H. D. WILLIAMS, *Phil. Mag.* **16** (1967) 849.
12. I. J. SPARK, D. M. R. TAPLIN, and G. J. COCKS, to be published (1969).
13. D. M. R. TAPLIN and A. L. WINGROVE, *Acta Met.* **15** (1967) 1231.
14. R. M. HAINES, UKAEA/TRG/116/W (1966).
15. W. W. MULLINS, and J. P. HIRTH, *J. Phys. Chem. Solids* **24** (1963) 1391.
16. K. FARRELL, B. T. M. LOH, and J. O. STIEGLER, *Trans. ASM* **60** (1967) 485.
17. J. A. MALCOLM and G. R. PURDY, *Trans. AIME* **239** (1967) 1391.
18. W. W. MULLINS and R. F. SEKERKA, *J. Appl. Phys.* **34** (1963) 323.